Pion-nucleon amplitude near threshold: the sigma-term and scattering lengths beyond few loops

S. Kondratyuk
TRIUMF, 4004 Wesbrook Mall, Vancouver, British Columbia, Canada V6T 2A3
(April 22, 2002)

Abstract

The pion-nucleon amplitude is considered in the vicinity of the elastic scattering threshold within a relativistic dynamical model dressing the πNN and $\pi N\Delta$ vertices self-consistently with an infinite number of meson loops. The dressing is formulated as solution of a system of coupled integral equations incorporating unitarity, crossing symmetry and analyticity constraints. The calculated scattering lengths and the sigma-term agree with recent data analyses. In this model multiple loops are significant both below and at threshold. The contribution of the Δ resonance is discussed, including effects of its dressing. A comparison with the approaches of chiral perturbation theory and the Bethe-Salpeter equation is outlined.

Typeset using REVTEX

I. INTRODUCTION

The pion-nucleon scattering amplitude near the physical threshold is an interesting object to study for a number of reasons. At the threshold point itself, the amplitude is proportional to the s-wave scattering lengths, whose values are known to be strongly constrained by chiral symmetry [1]. For the amplitude below threshold, one can establish other chiral low-energy theorems [2,3] involving such quantities as the nucleon sigma-term [4] and thus related to the pattern of the explicit chiral symmetry breaking of QCD [5]. To extract the sigma-term from scattering data one usually analyses the amplitude at the Cheng-Dashen point. Although corresponding to unphysical kinematics, this point is of special importance because there both pions are on-shell and the difference between the amplitude and the sigma-term is minimal [3,6,7].

Chiral perturbation theory has been used to study loop corrections to the low-energy theorems and, in particular, to calculate the sigma-term [8]. However, the near-threshold region is significantly affected by the presence of singularities which may make a non-relativistic perturbative expansion unreliable [9]. In general, the pion-nucleon amplitude is ill-defined (and hence non-analytic) at the Cheng-Dashen point and the threshold is a branch point dictated by unitarity. To obey unitarity for pion-nucleon scattering exactly, one can solve the relativistic Bethe-Salpeter equation with a tree-level potential; this yields a good description of the phase shifts and scattering lengths as well as allows one to calculate the sigma-term [10]. At the same time, the models based on the Bethe-Salpeter equation usually do not preserve crossing symmetry (however, see [11]) which plays an important role in the derivation of the low-energy theorems [3].

In the present paper the pion-nucleon amplitude is studied in the near-threshold region using a relativistic dynamical model which incorporates essential constraints from unitarity, analyticity and crossing symmetry. The effective lagrangian of the model includes pions, nucleons, the Δ resonance, the ρ and σ mesons. The main distinguishing feature of this approach is a special method of calculating pion-nucleon and other meson-baryon loop corrections to free propagators and bare vertices. An infinite series of loops is summed up by solving a system of coupled integral equations for the dressed vertices and propagators. These equations are formulated so that constraints from unitarity, crossing symmetry and analyticity are fulfilled. In particular, the nucleon and Δ propagators as well as the πNN and $\pi N\Delta$ vertices are dressed in a self-consistent way. This formalism was expounded in Refs. [12], where the treatment of the Δ was simplified in that the Δ propagator was dressed with only one πN loop and the $\pi N\Delta$ vertex was not dressed at all. In the present paper the dressed propagators of the nucleon and Δ as well as the dressed $\pi N\Delta$ and πNN vertices are calculated as a solution of one system of coupled integral equations. The dressing procedure of [12] was also extended to include photons while preserving gauge-invariance [13]. Unitarity of the coupled-channel S-matrix above threshold was ensured since the dressing is consistent with the application of the dressed vertices and propagators in the K-matrix approach. In this way a good description of intermediate-energy pion-nucleon scattering, pion photoproduction and Compton scattering was obtained, and the nucleon electromagnetic polarisabilities were calculated and found to be in agreement with experiment [14,15]. Since all parameters of the model (resonance coupling constants and the regularising cutoff) were fixed at the intermediate energies in Ref. [14], the present calculation of the pion-nucleon

amplitude below and at threshold is determined solely by the loop dynamics.

The outline of the paper is as follows. The pion-nucleon amplitude at threshold and at the Cheng-Dashen point is defined in Section II, where also relevant low-energy theorems are cited. The formalism of the model is described in Section III, where the integral equations for the dressed vertices and propagators and the method of their solution will be described. In Section IV the invariant pion-nucleon amplitudes in the near-threshold region are explicitly expressed via the dressed functions. The main results of the paper will be presented in that section. In particular, we will show that effects of multiple meson loops can be quite significant both below and at threshold. Also, the contribution of the Δ will be discussed, including the effects of the dressing of the $\pi N\Delta$ vertex. We will argue that the analyticity constraints incorporated in the dressing procedure are essential for the description of both the scattering lengths and the subthreshold coefficients in the same dynamical approach. Our formalism and results will be compared with the approaches of chiral perturbations theory and the Bethe-Salpeter equation in Section V. Concluding remarks are made in Section VI.

II. PION-NUCLEON AMPLITUDE NEAR THRESHOLD

The standard isospin decomposition of the pion-nucleon amplitude is [16]

$$M_{\alpha\beta} = \delta_{\alpha\beta} M^+ + \frac{1}{2}[\tau_\alpha, \tau_\beta] M^-, \tag{1}$$

where τ_α are Pauli matrices for the pion isospins. The spin structure of the amplitude is

$$M^\pm = \overline{u}(p') \left\{ A^\pm + \frac{\not{k}' + \not{k}}{2} B^\pm \right\} u(p) = \overline{u}(p') \left\{ D^\pm - \frac{1}{4m} [\not{k}', \not{k}] B^\pm \right\} u(p), \tag{2}$$

where k and k' (p and p') are the four-momenta of the initial and final pions (nucleons), respectively, and $u(p)$ is the Dirac four-spinor. The invariant amplitudes $A^\pm$, $B^\pm$, $D^\pm$ depend on the Mandelstam variables $s = (p+k)^2$, $u = (p-k')^2$ and $t = (k-k')^2$. We will also use the standard kinematic variables $\nu = (s-u)/(4m)$ and $\nu_B = (t - 2\mu^2)/(4m)$, where $m = 0.939$ GeV and $\mu = 0.138$ GeV are the nucleon and pion masses. The two sets of invariant functions in Eq. (2) are related as $D = A + \nu B$.

In the following we shall calculate the value of the pion-nucleon amplitude at the subthreshold Cheng-Dashen point, i.e. at $\nu = 0$, $t = 2\mu^2$, with both pions on shell, $k^2 = k'^2 = \mu^2$. One quantity of special interest is the sigma-term, which is related to the pion-nucleon amplitude at the Cheng-Dashen point as

$$\Sigma = F_\pi^2 \lim_{\nu \to 0} \overline{D}^+(\nu, t = 2\mu^2), \tag{3}$$

where $F_\pi = 92.4$ MeV is the pion decay constant. The bar indicates that the tree-level amplitude evaluated with the pseudovector πNN vertex (usually called the "pseudovector Born contribution") is subtracted,

$$\overline{B}^+ = B^+ - \frac{g^2}{m}\frac{\nu}{\nu_B^2-\nu^2}\,, \tag{4}$$

$$\overline{B}^- = B^- - \frac{g^2}{m}\left(\frac{\nu_B}{\nu_B^2-\nu^2} - \frac{1}{2m}\right)\,, \tag{5}$$

$$\overline{D}^+ = D^+ - \frac{g^2}{m}\frac{\nu_B^2}{\nu_B^2-\nu^2}\,, \tag{6}$$

$$\overline{D}^- = D^- - \frac{g^2}{m}\left(\frac{\nu\,\nu_B}{\nu_B^2-\nu^2} - \frac{\nu}{2m}\right). \tag{7}$$

We use the value $g = 13.02$ [17] for the πNN coupling constant (the physical masses and coupling constants of the particles used in this calculation are summarised in Table I). According to a chiral low-energy theorem [3], the sigma-term Eq. (3) at the Cheng-Dashen point equals the scalar form factor of the nucleon up to corrections of order $\mathcal{O}(\mu^4)$. The scalar form factor can be related to the explicit chiral symmetry breaking (see, e.g., Refs. [8,9]). Another low-energy theorem [2,3] concerns the amplitude D^-, requiring that the coefficient

$$C = 2F_\pi^2 \lim_{\nu\to 0}\frac{\overline{D}^-(\nu, t=2\mu^2)}{\nu} \tag{8}$$

should approach unity in the chiral limit (i.e. for a vanishing pion mass), up to corrections of order $\mathcal{O}(\mu^2)$.

In addition to the pion-nucleon amplitude in the subthreshold region, we shall also calculate the s-wave scattering lengths which characterise the amplitude at the threshold point $Th \equiv \{s = (m+\mu)^2, u = (m-\mu)^2, t = 0\}$:

$$a^{1/2} = \left.\frac{D^+ + 2D^-}{4\pi(1+\mu/m)}\right|_{Th}\,, \tag{9}$$

$$a^{3/2} = \left.\frac{D^+ - D^-}{4\pi(1+\mu/m)}\right|_{Th}\,, \tag{10}$$

corresponding to the total isospins 1/2 and 3/2, respectively. The low-energy theorem [1] asserts that at lowest order the numerators in Eqs. (9) and (10) equal $\mu/(F_\pi^2)$ and $-\mu/(2F_\pi^2)$, respectively.

III. DESCRIPTION OF THE MODEL

Our calculation of the near-threshold pion-nucleon amplitude is based on the approach of Refs. [12–14]. However, the treatment of the Δ resonance is significantly improved in the present version of the model, as will be explained in more detail below. In this section we describe our approach, focusing on the ingredients which are most relevant in the near-threshold region.

A. Structure of the amplitude

The πN amplitude below and at threshold is purely real. It this model it is constructed as the sum of the s-, u-channel nucleon and Δ exchange graphs, plus the t-channel ρ and σ meson exchange graphs,

$$M = M_s + M_u + M_s^\Delta + M_u^\Delta + M_t^{\rho\sigma}, \tag{11}$$

as shown in Fig. 1. These are not simple tree diagrams, but rather skeleton diagrams as they comprise *dressed* vertices and propagators. Being a solution of a system of coupled integral equations, the nucleon and Δ propagator and vertices are dressed with meson loops up to infinite order, while the ρ and σ propagators are calculated in a one $\pi\pi$ loop approximation. Thus the central element of the approach is the calculation of the dressed vertices and propagators, which will be described in the following.

B. Structure of dressed vertices and propagators of the nucleon and Δ

The πNN vertex required throughout the dressing procedure has only one of the nucleons off the mass shell with the other nucleon and the pion being on-shell (the so-called half-off-shell vertex). For an incoming off-shell nucleon with the four-momentum squared p^2, the most general Lorentz- and CPT-covariant structure of such a vertex is [19][1]

$$\tau_\alpha \Gamma(p) = \tau_\alpha \, \gamma^5 \Big[G_{PS}(p^2) + \frac{\not{p} + m}{2m} G_{PV}(p^2) \Big], \tag{12}$$

where $G_{PS,PV}(p^2)$ are pseudovector and pseudoscalar form factors, to be computed in Section III C below. The Lorentz-invariant expression for the nucleon self-energy is written in terms of two invariant functions $A(p^2)$ and $B(p^2)$,

$$\Sigma(p) = \Sigma_L(p) - (Z_2 - 1)(\not{p} - m) - Z_2 \, \delta m \ , \ \ \Sigma_L(p) = A(p^2) \not{p} + B(p^2) m \, , \tag{13}$$

where Σ_L denotes the loop contributions to the self-energy. The complete self-energy $\Sigma(p)$ contains also the counter-term contribution with renormalisation constants Z_2 and δm adjusted to provide the correct pole properties Eq. (32) of the dressed nucleon propagator [21]. The dressed nucleon propagator is written as

$$S(p) = \frac{1}{\not{p} - m - \Sigma(p)} = \frac{\not{p} + \xi(p^2)}{\alpha(p^2)[p^2 - \xi^2(p^2)]}, \tag{14}$$

where for later use we have introduced the self-energy functions

$$\alpha(p^2) = Z_2 - A(p^2), \quad \xi(p^2) = \frac{m B(p^2) + Z_2(m - \delta m)}{\alpha(p^2)}. \tag{15}$$

---

[1] We use the fully relativistic formalism, with the metric tensor, γ matrices and other general conventions of [20].

The nucleon self-energy will be calculated consistently with the πNN vertex in Section III C.

We choose the following form of the $\pi N\Delta$ vertex:

$$T_\alpha\, V_\mu(k,p) = T_\alpha\, \frac{\not{p} k_\mu - (p\cdot k)\gamma_\mu}{m_\Delta^2}\, F_{\pi N\Delta}((p-k)^2)\, G_\Delta(p^2), \tag{16}$$

where p and k are the 4-momenta of an incoming Δ and of an outgoing pion, respectively, and m_Δ is the mass of the Δ. The part $G_\Delta(p^2)$ of the form factor in Eq. (16) will be calculated in the dressing procedure described in Section III C. The function $F_{\pi N\Delta}((p-k)^2)$, depending on the nucleon momentum, is needed for convergence of the procedure. The isospin transition operators T_α are defined by the relations [22]

$$T_\alpha\, T_\beta^\dagger = \delta_{\alpha\beta} - \frac{\tau_\alpha \tau_\beta}{3}, \qquad T_\alpha^\dagger\, T_\alpha = 1. \tag{17}$$

To keep the calculations tractable, the $\pi N\Delta$ vertex in Eq. (16) is not chosen in the most general Lorentz-covariant form (for comparison, throughout the calculations we maintain the most general structure of the πNN vertex). It is important however that the vertex Eq. (16) has the property of "gauge-invariance" [23],

$$p\cdot V(k,p) = 0, \tag{18}$$

which allows one to eliminate the the background spin 1/2 component of the Δ propagator [24] and to keep only the spin 3/2 component

$$S_\Delta^{\mu\nu}(p) = \frac{1}{\not{p} - m_\Delta - \Sigma_\Delta(p)} \mathcal{P}_{3/2}^{\mu\nu}(p) = \frac{\not{p} + \omega(p^2)}{\eta(p^2)[p^2 - \omega^2(p^2)]}\, \mathcal{P}_{3/2}^{\mu\nu}(p), \tag{19}$$

where the spin 3/2 projection operator

$$\mathcal{P}_{3/2}^{\mu\nu}(p) = g^{\mu\nu} - \frac{\gamma^\mu\gamma^\nu}{3} - \frac{\not{p}\gamma^\mu p^\nu + p^\mu\gamma^\nu \not{p}}{3p^2}. \tag{20}$$

Formulae completely analogous to Eqs. (13,15) hold for the Δ self-energy also. Although treating the Δ as a pure spin 3/2 state does not improve the description of pion-nucleon scattering phase shifts as compared to the conventional treatment [10], it significantly simplifies the dynamical calculation of the Δ self-energy. For example, we need to compute only two self-energy functions $A_\Delta(p^2)$ and $B_\Delta(p^2)$, instead of 10 invariant functions [25] which would be required if the spin 1/2 background were not eliminated.

C. Integral equations for the dressing and their solution

The πNN form factors $G_{PV,PS}(p^2)$, the nucleon self-energy functions $A(p^2), B(p^2)$, the $\pi N\Delta$ form factor $G_\Delta(p^2)$ and the Δ self-energy functions $A_\Delta(p^2), B_\Delta(p^2)$ are calculated by solving a system of coupled integral equations. This amounts to dressing these two- and three-point Green's functions with meson loops up to infinite order. In the earlier version of the model [12–14] the Δ resonance was not treated completely consistently with the nucleon: the Δ self-energy was computed up to one πN loop only and the dressing of

the $\pi N\Delta$ vertex was not included. However, considering nucleon Compton scattering, we showed [15] that such simplified Δ dressing, while being generally adequate, can lead to problems at low energies. Therefore, in the present work we refine the dressing procedure so that the nucleon and Δ are now treated on the same footing.

The dressing equations will be formulated using the following notation. A generic Green's function $\mathcal{G}(q)$ is a sum of independent Lorentz-structures (e. g. 1, $\not{q}$, γ_μ, etc.), each of which is multiplied with a Lorentz-invariant function depending on q^2 (such as form factors or self-energy functions). If we use only imaginary or only real parts of the invariant functions, the result will be denoted as $\mathcal{G}_I(q)$ or $\mathcal{G}_R(q)$, respectively. If $\mathcal{G}(q)$ is calculated from a loop integral, then according to Cutkosky rules [26] $\mathcal{G}_I(q)$ is proportional to the discontinuity of the integral across the unitary cut (due to the pinching poles of the propagators in the integrand) in the complex q^2 plane, and $\mathcal{G}_R(q)$ is the principal-value part of the integral[2].

In our case, the principal-value and pole parts of the dressed half-off-shell πNN vertex are denoted as $\Gamma_R(p)$ and $\Gamma_I(p)$, respectively. The expression for $\Gamma_R(p)$ or $\Gamma_I(p)$ is obtained by substituting, respectively, only the real or only the imaginary parts of the form factors $G_{PV,PS}(p^2)$ in the right-hand side of Eq. (12). The same applies to the $\pi N\Delta$ vertex Eq. (16): to obtain $(V_\mu)_R(k,p)$ or $(V_\mu)_I(k,p)$ we use only $\mathrm{Re}G_\Delta(p^2)$ or $\mathrm{Im}G_\Delta(p^2)$, respectively. Similarly, the pole part $\Sigma_I(p)$ of the nucleon self-energy Eq. (13) contains only $\mathrm{Im}A(p^2)$ and $\mathrm{Im}B(p^2)$, and the principal-value part $\Sigma_R(p)$ only $\mathrm{Re}A(p^2)$ and $\mathrm{Re}B(p^2)$. The pion propagator $D(k) = [k^2 - \mu^2 + i0]^{-1}$ does not get dressed, therefore its imaginary part comes from the on-shell pions: $D_I(k) = \delta(k^2-\mu^2)\theta(k_0)$. In the same way, we retain only the dominant pole contribution to the discontinuity of the nucleon propagator: $S_I(p) = (\not{p}+m)\delta(p^2-m^2)\theta(p_0)$. The resonance propagators do not have poles on the physical Riemann sheet, so their discontinuous parts come solely from their self-energies. For example, the discontinuity of the dressed Δ propagator Eq. (19) is obtained by keeping only the imaginary parts of its invariant functions:

$$(S_\Delta^{\mu\nu})_I(p) = \left\{ \not{p}\,\mathrm{Im}\frac{1}{\eta(p^2)[\,p^2-\omega^2(p^2)\,]} + \mathrm{Im}\frac{\omega(p^2)}{\eta(p^2)[\,p^2-\omega^2(p^2)\,]} \right\}\theta(p_0)\,, \tag{21}$$

and analogously for the ρ and σ mesons (unlike the Δ, however, the propagators of the meson resonances are dressed in a one $\pi\pi$ loop approximation only, as will be discussed in more detail below and in Appendix A).

With the introduced notation, the system of dressing equations can be written

$$\begin{aligned}
\Gamma_I(p) = {} & \frac{1}{8\pi^2}\int d^4k\,\Gamma_R(p'-k)S(p'-k)\overline{\Gamma}_R(p'-k)S_I(p-k)D_I(k)\Gamma_R(p) \\
& + \frac{1}{6\pi^2}\int d^4k\,(V_\mu)_R(-k,p'-k)S_\Delta^{\mu\nu}(p'-k)(\overline{V}_\nu)_R(-q,p'-k) \\
& \qquad \times S_I(p-k)D_I(k)\Gamma_R(p) \\
& - \frac{1}{6\pi^2}\int d^4k\,\Gamma_R(p'-k)S(p'-k)(V_\mu)_R(q,p-k)(S_\Delta^{\mu\nu})_I(p-k)
\end{aligned}$$

---

[2]If the theory obeys analyticity (causality) constraints, the pole and principal-value parts of a loop must be related to each other through a dispersion integral [27].

$$\times D_I(k)(\overline{V}_\nu)_R(k,p-k) \;+\; \Gamma_I^{\rho\sigma}(p)\;, \tag{22}$$

$$\mathrm{Re}\left\{\begin{matrix} G_{PV} \\ G_{PS}\end{matrix}\right\}(p^2) = \left\{\begin{matrix} G^0_{PV} \\ G^0_{PS}\end{matrix}\right\}(p^2) + \frac{\mathcal{P}}{\pi}\int_{(m+\mu)^2}^{\infty} dp'^2\,\frac{\mathrm{Im}\left\{\begin{matrix} G_{PV} \\ G_{PS}\end{matrix}\right\}(p'^2)}{p'^2-p^2}\;, \tag{23}$$

$$\Sigma_I(p) = -\frac{3}{8\pi^2}\overline{\Gamma}_R(p)\int d^4k\, S_I(p-k)D_I(k)\Gamma_R(p)\;, \tag{24}$$

$$\mathrm{Re}\left\{\begin{matrix} A \\ B\end{matrix}\right\}(p^2) = \frac{\mathcal{P}}{\pi}\int_{(m+\mu)^2}^{\infty} dp'^2\,\frac{\mathrm{Im}\left\{\begin{matrix} A \\ B\end{matrix}\right\}(p'^2)}{p'^2-p^2}\;, \tag{25}$$

$$\begin{aligned}(V_\mu)_I(q,p) = {}& \frac{1}{4\pi^2}\int d^4k\,\Gamma_R(p'-k)S(p'-k)\overline{\Gamma}_R(p'-k)S_I(p-k) \\ & \times D_I(k)(V_\mu)_R(k,p) \\ & + \frac{1}{24\pi^2}\int d^4k\,(V_\nu)_R(-k,p'-k)S_\Delta^{\nu\lambda}(p'-k)(\overline{V}_\lambda)_R(-q,p'-k) \\ & \times S_I(p-k)D_I(k)(V_\mu)_R(k,p) \;+\; (V_\mu^{\rho\sigma})_I(q,p)\;,\end{aligned} \tag{26}$$

$$\mathrm{Re}G_\Delta(p^2) = G^0_\Delta(p^2) + \frac{\mathcal{P}}{\pi}\int_{(m+\mu)^2}^{\infty} dp'^2\,\frac{\mathrm{Im}G_\Delta(p'^2)}{p'^2-p^2}\;, \tag{27}$$

$$\Sigma_I^\Delta(p) = \frac{\mathcal{P}^{\nu\mu}_{3/2}(p)}{16\pi^2}\int d^4k\,(\overline{V}_\mu)_R(k,p)S_I(p-k)D_I(k)(V_\nu)_R(k,p)\;, \tag{28}$$

$$\mathrm{Re}\left\{\begin{matrix} A_\Delta \\ B_\Delta\end{matrix}\right\}(p^2) = \frac{\mathcal{P}}{\pi}\int_{(m+\mu)^2}^{\infty} dp'^2\,\frac{\mathrm{Im}\left\{\begin{matrix} A_\Delta \\ B_\Delta\end{matrix}\right\}(p'^2)}{p'^2-p^2}\;, \tag{29}$$

where $\mathcal{P}$ denotes taking the principal-value of an integral, and the isospin factors have been absorbed in the coefficients on the right-hand side. The inhomogeneities $\Gamma_I^{\rho\sigma}(p)$ in Eq. (22) and $(V_\mu^{\rho\sigma})_I(q,p)$ in Eq. (26) contain ρ and σ mesons, as described in Appendix A. The real functions $G^0_{PV,PS}(p^2)$ and G^0_Δ are bare πNN and $\pi N\Delta$ form factors, respectively. To see that the system of dressing equations is neither under- nor over-determined, note that Eqs. (22,24) and (28) have two independent spinor structures each. Thus Eqs. (22-29) are 14 scalar equations for 14 scalar functions $\mathrm{Im}G_1(p^2)$, $\mathrm{Im}G_2(p^2)$, $\mathrm{Im}A(p^2)$, $\mathrm{Im}B(p^2)$, $\mathrm{Re}G_1(p^2)$, $\mathrm{Re}G_2(p^2)$, $\mathrm{Re}A(p^2)$, $\mathrm{Re}B(p^2)$, $\mathrm{Im}G_\Delta(p^2)$, $\mathrm{Im}A_\Delta(p^2)$, $\mathrm{Im}B_\Delta(p^2)$, $\mathrm{Re}G_\Delta(p^2)$, $\mathrm{Re}A_\Delta(p^2)$, $\mathrm{Re}B_\Delta(p^2)$.

Formally, Eqs. (22-29) constitute a coupled system of nonlinear integral equations. Despite its quite complicated analytic form, this system of equations has a rather transparent meaning. The diagrammatic representation of the dressing equations is shown in Fig. 2. The equations are solved by iteration, starting with input bare form factors $G^0_{PV,PS}$, G^0_Δ. In the course of iteration one effectively sums up an infinite series of meson-loop corrections to the bare vertices and free propagators. At each iteration step we first calculate the discontinuities of the loop integrals through the Cutkosky rules; these pole parts are then used in dispersion integrals to compute the corresponding principal-value parts. The details of the computation technique can be found in [12,13]. Here we will recapitulate only the most important points and discuss the new issues arising due to the consistent incorporation of

the Δ resonance in the dressing procedure.

The use of bare form factors $G^0_{PV,PS}(p^2)$ and G^0_Δ is necessary to regularise the equations[3]. We choose the purely pseudovector structure for the bare πNN vertex, i. e. $G^0_{PS}(p^2) = 0$, since the derivative coupling of pions at low-energies is dictated by chiral symmetry. The bare πNN from factor is chosen in the form

$$G^0_{PV}(p^2) = f\ \exp\left[-\ln 2\frac{(p^2-m^2)^2}{\Lambda_N^4}\right], \tag{30}$$

where Λ_N^2 is a half-width. The bare coupling constant $f \equiv f_{\pi NN}$ is adjusted so that the dressed πNN vertex is normalised on-shell to the physical πNN coupling constant:

$$\lim_{\not p \to m} \Gamma(p) = g\,\gamma^5\,, \tag{31}$$

where the "sandwich" between the spinors of the initial and final nucleons is implicit. The usual renormalisation [21] of the dressed nucleon propagator

$$\lim_{\not p \to m} S(p) = \frac{1}{\not p - m} \tag{32}$$

is imposed by adjusting the field renormalisation constant $Z_2 \equiv Z_2^N$ and the mass shift $\delta m \equiv \delta m_N$ (see Eqs. (13) and (14)). The renormalisation of the $\pi N\Delta$ vertex and Δ propagator is done similarly, except that now the pole properties are required of a propagator with only the real parts of the self-energy functions [26,12]. There are three corresponding renormalisation constants: $f_{\pi N\Delta}$, Z_2^Δ and δm_Δ. Note that, due to the coupled nature of the dressing equations (22-29), the six renormalisation conditions for the vertices and propagators can be obeyed only simultaneously. Thus $f_{\pi NN}$, Z_2^N, δm_N, and $f_{\pi N\Delta}$, Z_2^Δ, δm_Δ are interdependent. The complete set of renormalisation constants obtained in the calculation are given in Table II.

We stress that the half-width Λ_N^2 is not a completely independent parameter; the iteration procedure converges only for $\Lambda_N^2 < (\Lambda_N^{max})^2$, and it is important that $(\Lambda_N^{max})^2$ is much larger than the energy scale due to the explicitly included particles (with the set of parameters used in this calculation, $(\Lambda_N^{max})^2 \approx 3$ GeV^2). When a convergent solution does exist, it is reached in practice after about 30 iteration steps for $\Lambda_N^2 \approx (\Lambda_N^{max})^2$. The bare $\pi N\Delta$ form factor $G^0_\Delta(p^2_\Delta)$ as well as of the form factors $F_{\pi N\Delta}(p^2_N)$, $F_{\rho\pi\pi}(p^2_\rho)$, $F_{\sigma\pi\pi}(p^2_\sigma)$, $F_{\rho NN}(p^2_N)$ and $F_{\sigma NN}(p^2_N)$, appearing in the vertices with the resonances, have the same exponential form as Eq. (30), but peak at the masses of corresponding particles (see Appendix A). We assume the width Λ_R^2 of these bare form factors to be the same for all resonances, and set it to the maximal value allowed by the convergence requirement. This is done in keeping with the general emphasis of our approach on the loop dynamics as determined by the dressing rather than on fitting additional parameters. Ideally, values of Λ_R^2 for different meson resonances

---

[3]An attempt to get rid of the bare form factors by using subtracted dispersion integrals in Eqs. (23,25,27,29) fails since each new iteration step would require more subtractions than the previous.

should come from dynamical dressing of these mesons consistently with the nucleon and the Δ. Such an extension of the present approach is certainly feasible, although has not been done yet.

The effects of the loop corrections on the πNN vertex are similar to those discussed in detail in [12,14], where the Δ was not dressed consistently. We mention the main points here. The dressing generates an energy-dependent admixture of the pseudoscalar coupling, which at low energies remains much smaller than the pseudovector component (in agreement with chiral symmetry requirements) but becomes more prominent at intermediate energies. The pseudovector form factor in narrowed by the dressing. This softening persists independently of the functional form of the bare form factor, provided the latter falls sufficiently fast at infinity, and is stronger for wider bare form factors. Like the half-width Λ_N^2 of the bare πNN form factor, the coupling constants $g_{\rho NN}$, κ_ρ, $g_{\sigma NN}$, $g_{\sigma\pi\pi}$ and $f_{\sigma\pi\pi}$ of the ρ and σ mesons are also mutually constrained by the requirement that a convergent solution of the dressing equations exist. The remaining freedom in the parameters was removed by calculating the pion-nucleon phase shifts using the dressed K-matrix approach [14] and comparing them with data analyses [28] at intermediate energies. The parameters from [14] are reproduced in Table III. As long as the iteration procedure converges, the description of the phase shifts is largely independent of the width of the bare form factor [12]. The usage of the exponential bare form factor is also not essential and dipole-like bare form factors lead to similar dressed vertices. We emphasise that in fixing the parameters in [14] we did not use any results of data analyses for the scattering lengths or for the subthreshold amplitudes. Therefore there are *no free parameters* in the present calculation of the near-threshold amplitudes.

IV. SCATTERING AMPLITUDE IN TERMS OF THE DRESSED VERTICES AND PROPAGATORS

Having solved the dressing equations, we proceed to evaluate the invariant amplitudes $A^\pm$ and $B^\pm$, introduced in Eq. (2). First we write the s- and u-channel diagrams in Eq. (11) in terms of the dressed πNN and $\pi N\Delta$ vertices Eqs. (12,16) and dressed nucleon and Δ propagators Eqs. (14,19). Then we add the t-channel diagrams written in terms of the the relevant meson vertices and propagators Eqs. (A3,A5,A10,A14,A15,A21). Note that at the considered kinematics, only the real parts of the invariant functions of the two- and three-point Green's functions enter in the amplitude. After doing some straightforward algebra, the contribution of the nucleon, ρ and σ exchange diagrams to the invariant amplitudes can be written as

$$
\begin{aligned}
A^+ = & \frac{G_{PS}^2(s)[\xi(s)-m] + \dfrac{G_{PS}(s)G_{PV}(s)}{m}[s-m^2] + \dfrac{G_{PV}^2(s)}{4m^2}[m+\xi(s)][s-m^2]}{\alpha(s)[s-\xi^2(s)]} \\
& + \frac{G_{PS}^2(u)[\xi(u)-m] + \dfrac{G_{PS}(u)G_{PV}(u)}{m}[u-m^2] + \dfrac{G_{PV}^2(u)}{4m^2}[m+\xi(u)][u-m^2]}{\alpha(u)[u-\xi^2(s)]} \\
& - \frac{g_{\sigma NN}F_{\sigma\pi\pi}(t)\left[g_{\sigma\pi\pi}\mu - f_{\sigma\pi\pi}\dfrac{k'^2+k^2-t}{2\mu}\right]}{Z^\sigma\,[t-\zeta^2(t)]},
\end{aligned}
\tag{33}
$$

$$A^- = \frac{G_{PS}^2(s)[\xi(s)-m] + \frac{G_{PS}(s)G_{PV}(s)}{m}[s-m^2] + \frac{G_{PV}^2(s)}{4m^2}[m+\xi(s)][s-m^2]}{\alpha(s)[s-\xi^2(s)]}$$
$$- \frac{G_{PS}^2(u)[\xi(u)-m] + \frac{G_{PS}(u)G_{PV}(u)}{m}[u-m^2] + \frac{G_{PV}^2(u)}{4m^2}[m+\xi(u)][u-m^2]}{\alpha(u)[u-\xi^2(s)]}$$
$$+ \frac{g_{\rho NN} g_{\rho\pi\pi} \kappa_\rho F_{\rho\pi\pi}(t)(u-s)}{2mZ^\rho\,[t-\lambda^2(t)]}, \tag{34}$$

$$B^+ = -\frac{G_{PS}^2(s) + \frac{G_{PS}(s)G_{PV}(s)}{m}[m+\xi(s)] + \frac{G_{PV}^2(s)}{4m^2}[m^2+s+2m\xi(s)]}{\alpha(s)[s-\xi^2(s)]}$$
$$+ \frac{G_{PS}^2(u) + \frac{G_{PS}(u)G_{PV}(u)}{m}[m+\xi(u)] + \frac{G_{PV}^2(u)}{4m^2}[m^2+u+2m\xi(u)]}{\alpha(u)[u-\xi^2(u)]}, \tag{35}$$

$$B^- = -\frac{G_{PS}^2(s) + \frac{G_{PS}(s)G_{PV}(s)}{m}[m+\xi(s)] + \frac{G_{PV}^2(s)}{4m^2}[m^2+s+2m\xi(s)]}{\alpha(s)[s-\xi^2(s)]}$$
$$- \frac{G_{PS}^2(u) + \frac{G_{PS}(u)G_{PV}(u)}{m}[m+\xi(u)] + \frac{G_{PV}^2(u)}{4m^2}[m^2+u+2m\xi(u)]}{\alpha(u)[u-\xi^2(u)]}$$
$$+ \frac{g_{\rho NN} g_{\rho\pi\pi}(1+\kappa_\rho) F_{\rho\pi\pi}(t)}{Z^\rho\,[t-\lambda^2(t)]}. \tag{36}$$

The contribution of the Δ exchange in Eq. (11) is given by (restoring the isospin indices)

$$(M_s^\Delta)_{\alpha\beta} = \left(\delta_{\alpha\beta} - \frac{\tau_\alpha\tau_\beta}{3}\right) \frac{G_\Delta^2(s)}{m_\Delta^4\,\eta(s)[s-\omega^2(s)]} \overline{u}(p') \left[(\not p' + \not k')k'_\mu - (p'+k')\cdot k'\,\gamma_\mu\right]$$
$$\times [\not p + \not k + \omega(s)]\,\mathcal{P}_{3/2}^{\mu\nu}(p+k)\,[(\not p + \not k)k_\nu - (p+k)\cdot k\,\gamma_\nu]\,u(p) \tag{37}$$

$$(M_u^\Delta)_{\alpha\beta} = \left(\delta_{\alpha\beta} - \frac{\tau_\beta\tau_\alpha}{3}\right) \frac{G_\Delta^2(u)}{m_\Delta^4\,\eta(u)[u-\omega^2(u)]} \overline{u}(p')\,[-(\not p' - \not k)k_\mu + (p'-k)\cdot k\,\gamma_\mu]$$
$$\times [\not p - \not k' + \omega(u)]\,\mathcal{P}_{3/2}^{\mu\nu}(p-k')\,[-(\not p - \not k')k'_\nu + (p-k')\cdot k'\,\gamma_\nu]\,u(p)\,. \tag{38}$$

As we shall see below, the contribution of the Δ is rather small near threshold, and so we will not give the quite lengthy explicit decomposition of Eqs. (37,38) in terms of the invariant amplitudes.

Properties of analyticity and crossing symmetry

Due to the use of the cutting rules and dispersion integrals in the formulation of Eqs. (22-29), the two- and three-point Green's functions obtained by solving these equations possess correct analyticity structure associated with the nucleon and Δ exchanges and obey the two-body (πN) unitarity. Furthermore, the πN amplitude obeys the crossing symmetry requirements that A^+, $A^-/(s-u)$, $B^+/(s-u)$ and B^- be invariant under the replacement $s \leftrightarrow u$. The crossing is respected due to our using the dressed two- and three-point Green's

functions in *both* s- and u-type diagrams. At the same time, the t-channel analyticity structure is not fully reproduced because the t-channel cuts are taken into account only through the $\pi\pi$ loops in the ρ and σ propagators but the loop corrections to the vertices with the ρ and σ mesons are not included. Also, the four-point one-particle irreducible diagrams – such as the box graph – are not included in the dressing.

The omitted dressed one-particle irreducible four-point diagrams can be thought of as being of order $\mathcal{O}(a^2)$ in a certain formal expansion, where the parameter a characterises the level of analyticity violation in the model [14]. In this expansion, the lowest order $\mathcal{O}(a^0)$ corresponds to an amplitude with no dressing, in which case the violation of analyticity in maximal. The next order $\mathcal{O}(a^1)$ corresponds to an amplitude in which the one-particle reducible (with respect to the s-channel cuts) graphs contain the dressed propagators and vertices. Thus, at order $\mathcal{O}(a^1)$ analyticity is restored at the level of two- and three-point Green's functions, as is done in present dressing procedure. This can be quantified by defining the parameter a as in the following example. If a scattering amplitude $T(\omega)$ of a process can be represented at small energies ω as a power series

$$T(\omega) = c_0 + c_1\omega + c_2\omega^2 + \ldots , \tag{39}$$

then the coefficients c_i could, in principle, be computed *using the same model* but in two different ways:

1. Low-energy (LE) evaluation: compute $c_i(LE)$ by evaluating $T(\omega)$ directly at low energies;

2. Sum-rule (SR) evaluation: compute $c_i(SR)$ by calculating appropriate total cross sections and integrating them in the sum rules correspond to each particular coefficient.

These two ways of evaluation should give identical coefficients $c_i(LE) = c_i(SR) = c_i$ provided the analyticity of the model is exact. Such an ideal situation would correspond to the case with the "analyticity violation parameter" $a = 0$. In practical calculations there will always be discrepancies between the two above computation methods, which can be used to estimate the violation of analyticity in the model. Therefore one can define the parameter a as

$$a \sim |c_i(LE) - c_i(SR)| , \tag{40}$$

where the choice of a particular coefficient from the series Eq. (39) could be decided by additional considerations. This idea was tested for nucleon Compton scattering in Ref. [15], where the coefficients c_1 and $c_{2,3}$ are related to the anomalous magnetic moment and to nucleon polarisabilities, respectively. The proposed formal expansion in the parameter a can offer a systematic way of improving analyticity properties of dynamical approaches applicable at low and intermediate energies.

The properties of analyticity and crossing symmetry are crucial for the model to provide a good description of the amplitude both below and at the physical threshold[4]. To study

[4]A similar conclusion was reached in the framework of the relativistic baryon chiral perturbation theory [9], where it was pointed out that the standard low-energy expansion does not reproduce the correct analyticity structure in the vicinity of singularities.

this in more detail, we shall focus below on the sigma-term, the Adler-Weisberger coefficient C, as defined by Eqs. (3,8), and on the scattering lengths, as defined by Eqs. (9,10). We will collectively call these quantities "the near-threshold coefficients".

Near-threshold coefficients

The sigma-term and coefficient C at the Cheng-Dashen point

On expanding the amplitudes in Eqs. (33-38) around the Cheng-Dashen point $s = u = m^2, t = 2\mu^2$ (with $k^2 = k'^2 = \mu^2$) and using the definitions Eqs. (3,8), we obtain explicit formulae for the sigma-term and for the coefficient C in terms of the dressed vertices and propagators:

$$\Sigma = -F_\pi^2 \left\{ \frac{G_{PS}^2(m^2)}{m\,\alpha(m^2)} + \frac{g_{\sigma NN}\, g_{\sigma\pi\pi}\, \mu F_{\sigma\pi\pi}(2\mu^2)}{Z^\sigma\,[\,2\mu^2 - \zeta^2(2\mu^2)\,]} \right\} + \Sigma_\Delta, \tag{41}$$

$$C = 2F_\pi^2 \left\{ \frac{G_{PS}(m^2)}{\alpha(m^2)} \left[\frac{g}{m^2} - 4G'_{PS}(m^2) \right] - \frac{G_{PS}^2(m^2)}{2\alpha^2(m^2)} \left[\frac{1}{m^2} - 4\alpha'(m^2) \right] \right.$$
$$\left. + \frac{g_{\rho NN}\, g_{\rho\pi\pi}(1-\kappa_\rho) F_{\rho\pi\pi}(2\mu^2)}{Z^\rho\,[\,2\mu^2 - \lambda^2(2\mu^2)\,]} \right\} + C_\Delta, \tag{42}$$

where Σ_Δ and C_Δ contain the effects of the Δ exchange in the s- and u-channel diagrams and are given in Appendix B. In Eqs. (41) and (42) we have made use of the relations

$$\xi(m^2) = m, \quad \xi'(m^2) = \frac{\alpha(m^2) - 1}{2\,m\,\alpha(m^2)}, \quad G_{PS}(m^2) + G_{PV}(m^2) = g, \tag{43}$$

which follow from the renormalisation conditions Eqs. (31,32).

Due to the presence of a scalar component in the $\sigma\pi\pi$ vertex Eq. (A14) the σ t-channel exchange gives the dominant numerical contribution to the sigma-term. The ρ meson plays a similar role for the coefficient C. However, such a separation of Eqs. (41,42) into "nucleon contributions", "meson contributions" and "Δ contributions" can only be regarded as formal here: as already mentioned, Eqs. (22-29) not only determine the nucleon and Δ dressing, but also strongly constrain the other parameters of the model. For example, an arbitrary change of the values of the ρ and σ coupling constants would formally change the dominant contributions in Eqs. (41,42), but with these altered coupling constants the dressing procedure would not converge at all! In what follows we will discuss various ingredients of the dressing by comparing the "Dressed" and "Bare" calculations. The former contains the full dressing with the meson loops whereas in the latter the bare vertices and free propagators have been used (note that since the $\rho\pi\pi$, ρNN, $\sigma\pi\pi$ and σNN vertices do not get dressed in the model, in both calculations they are equipped with the bare form factors $F_{\pi N\Delta}(p_N^2)$, $F_{\rho\pi\pi}(p_\rho^2)$, $F_{\sigma\pi\pi}(p_\sigma^2)$, $F_{\rho NN}(p_N^2)$ and $F_{\sigma NN}(p_N^2)$, as defined in Appendix A). The obtained values of the near-threshold coefficients are summarised in Table IV. Results of several data analyses are quoted in the last column. Various ingredients of the fully dressed calculation are given in the other columns and will be discussed below in more detail.

Eqs. (41) and (42) show that the subthreshold parameters Σ and C are sensitive to the values and derivatives of of the πNN form factors and of the nucleon self-energy at

the nucleon pole. These low-energy features of the dressing are determined mainly by the imposition of the requirements of analyticity in formulation of the dressing Eqs. (22-29). To check that our results are determined mainly by the loop dynamics rather than by details of the bare form factor, we did another calculation, with the width of the bare form factor $\Lambda_N^2 = 2.8$ GeV^2 (which is near the upper limit $(\Lambda_N^2)^{max}$ dictated by the convergence) and all the other parameters were kept as given in Table III. As was shown in [12], despite using a much wider form factor, such a calculation leads to intermediate-energy phase shifts which are very similar to those obtained in the basic calculation with $\Lambda_N^2 = 1.8$ GeV^2. The near-threshold coefficients also are almost unaffected by this variation of the bare width: the sigma-term and the coefficient C change by less than 3%. This may serve as an estimate of the theoretical error in our calculations. Unlike the bare form factor, the the dressing itself is quite significant, as can be seen be comparing columns "Dressed" and "Bare" in Table IV.

Pion-nucleon scattering lengths

The scattering lengths are evaluated by substituting the explicit expressions for the amplitudes Eqs. (33–38) into Eqs. (9) and (10). The obtained values are listed in Table IV for the different calculations considered. The large effect of the dressing on $a^{1/2}$, in comparison with the small effect on $a^{3/2}$, is a reflection of the nucleon s-channel graph being influenced by the dressing more than the u-channel graph. Similarly to the subthreshold coefficients Σ and C, the scattering lengths are largely insensitive to the details of the bare form factor.

Role of the Δ resonance

Δ *pole contribution*

By the Δ contribution to the pion-nucleon amplitudes one usually understands the contribution of the s- and u-channel Δ exchange diagrams. This definition may be used for a comparison of our results with those of the chiral perturbation theory, where the Δ is usually not included as an explicit field in the lagrangian and thus does not appear in the loops [32,33,9][5]. By comparing the columns "Dressed" and "No Δ poles" in Table IV, we see that the pole contribution of the Δ is small both below and at threshold (the explicit formulae are given in Appendix B). For example, it changes the sigma-term by 0.26 MeV, which is somewhat smaller than the values typically found in other calculations [7,9,35]. However, a quantitative comparison of our results with other approaches should be carried

[5]There exist approaches [34] including the Δ explicitly in chiral lagrangians, in which case the Δ does enter in the loops. Such extensions of the standard chiral perturbation theory will not be discussed here.

out carefully since typically one retains the spin 1/2 background contribution to the Δ propagator (see, e. g., [32,9]). By contrast, in this model we deal with the pure spin 3/2 Δ due to the gauge-invariant structure of the $\pi N\Delta$ vertex Eq. (16).

Effects of the dressing of the $\pi N\Delta$ vertex

In addition to the s- and u-channel exchanges, the Δ resonance enters in the loop corrections to the πNN and $\pi N\Delta$ vertices, which are dressed up to infinite order. Such a contribution of the Δ through dressing has not been considered before in the context of the near-threshold πN amplitude. Due to the coupled nature of Eqs. (22-29), the Δ dressing affects the πN amplitude both directly and through its effects on the πNN vertex and nucleon propagator.

In the subthreshold region, the value of the sigma-term is slightly decreased by the Δ dressing, as can be seen by comparing the columns labelled "Dressed" and "Bare Δ" in Table IV (in the latter calculation the bare $\pi N\Delta$ vertex and the free Δ propagator were used). Comparison of these results with the column "No Δ poles" shows that the dressing moderates the small pole contribution of the Δ to the sigma-term even further. Notably, the effect of the consistent Δ dressing is to decrease the sigma-term and to increase the coefficient C, whereas the Δ exchange has the opposite effect. This suggests that meson loops should be treated with special care in dynamical calculations of the Δ contribution to the subthreshold πN amplitude.

Effects of multiple loops

The two- and three-point functions obtained as a solution of Eqs. (22-29) comprise an infinite series of meson-loop corrections. The effect of multiple meson loops on the near-threshold amplitude can be seen from column "One loop" in Table IV. This is a calculation in which the πNN and $\pi N\Delta$ vertices, as well as the nucleon, Δ, ρ and σ self-energies, include only one-loop corrections. These vertices and self-energies are obtained by iterating Eqs. (22-29) *only once* after discarding from them the effective two-loop contributions (the latter are the integrals containing one of the cut resonance propagators $(S^{\mu\nu}_{\Delta})_I$, $(D^{\mu\nu}_{\rho})_I$ or $(D_{\sigma})_I$). To focus on the genuine effects of the loops, no parameters were readjusted in this calculation, except the renormalisation constants $f \equiv f_{\pi NN}$, $f_{\pi N\Delta}$, $Z_2 \equiv Z_2^N$, Z_2^{Δ}, $\delta m \equiv \delta m_N$, δm_{Δ}. Note that in this case the πN scattering amplitude is not exactly an amplitude including only one-loop corrections to the tree-level approximation. Nevertheless, taking into account that most of the effects of the dressing are due to the loop corrections in the vertices, the difference of the thus defined "one loop" calculation from the fully dressed calculation can serve as a reasonable estimate of the effects beyond few perturbative loop corrections in the amplitude. Table IV shows that the multiple-loop effects are significant in the near-threshold region. In particular, these effects can be larger than the contribution of the Δ resonance which is traditionally assumed to be a leading correction to one-loop calculations. It is also noteworthy that the scattering lengths are rather sensitive to the effects of multiple loops while being completely unaffected by the Δ.

V. COMPARISON WITH THE APPROACHES OF CHIRAL PERTURBATION THEORY AND THE BETHE-SALPETER EQUATION

The near-threshold parameters obtained in this model are compared in Table V with calculations in chiral perturbation theory (χPT) and with those based on the Bethe-Salpeter equation (BSE). We quote the results of the heavy-baryon and relativistic (with the infrared regularisation) baryon formulations of chiral expansions, referred to as HBχPT and RBχPT, respectively. There is some similarity between the present model and the other approaches, as well as a number of differences. In principle, it would be desirable to compare the loops calculated in this model with the chiral loops and with the loops generated by the BSE at the most elementary level, i. e. by analysing the expansions of a simple Green's function such as the nucleon self-energy. However, such a comparison is hardly meaningful as in general the Green's functions are model- and representation-dependent in perturbative as well as nonperturbative approaches (see, e.g., [36] and references therein). Therefore, we will use a comparison of the near-threshold parameters in Table V to illustrate the most important similarities and differences between the four approaches: the present model, HBχPT, RBχPT and the BSE.

The basic dynamical degrees of freedom in all these approaches are the nucleon and the pion. However, unlike the two chiral formalisms, the present model and the BSE include the Δ resonance and the ρ and σ mesons explicitly. In general, these degrees of freedom give important contributions to the dressed Green's functions. In chiral approaches effects of the resonances are typically encapsulated in low-energy constants using a resonance-saturation hypothesis [32,37] (as mentioned above, extensions of the chiral expansion with the Δ as an explicit degree of freedom [34] are not discussed here). In our model, as well as in χPT, the πNN vertex is predominantly pseudovector at low-energies, which is a consequence of the spontaneous chiral symmetry breaking. A small pseudoscalar component in the vertex is associated with an explicit symmetry breaking. In all four approaches, the nontrivial dependence of the amplitudes on kinematical variables is determined by loop expansions. The methods of organising the expansions are different however, as are the methods of evaluating the loop diagrams.

The chiral expansions are series in small pion mass and momenta [38]. In the presence of a nucleon, a one-to-one correspondence is established in the (nonrelativistic) HBχPT between the power of each term in the expansion and the number of pion loops required for its calculation [39]. This nonrelativistic expansion is well-behaved in the part of the low-energy region which is not too close to the singularities of the amplitude dictated by unitarity and analyticity. However, it is necessary to rearrange the chiral expansion in order to calculate the amplitude near the singularities. This is most efficiently done in RBχPT [9] by using an infrared regularisation in the relativistic formalism and representing the amplitude through dispersion integrals. (Within HBχPT, the correct singularity structure can be captured only by summing an infinite number of loop corrections.) The main emphasis of the approach of the BSE is on obeying unitarity in the relativistic formalism [40,10]. The necessary loops are summed up effectively by solving the linear integral equation for the scattering amplitude. However, due to the use of a simplified kernel in practical calculations, the BSE does not yield a crossing symmetric amplitude.

The unitarity, crossing and analyticity constraints are used as the governing principle for

organising the meson-loop expansion in the present model. The dressing equations represent a self-consistent procedure of using cutting rules and dispersion relations. By solving them we effectively sum up an infinite series of loop diagrams in such a way that the essential singularity structure of the two- and three-point Green's functions is correctly reproduced. Results of this paper show that the ability of a dynamical calculation to describe both pion-nucleon scattering lengths and such subthreshold parameters as Σ and C depends crucially on whether it incorporates the analyticity constraints. However, in contrast to the chiral expansions or the BSE, one-particle irreducible four-point loop diagrams (such as the triangle or box graphs discussed in [9]) are not calculated explicitly in our model, which entails a violation of analyticity structure in the t-channel. Also, in this model we need to compute the dressed vertices only in the s- and u-type diagrams, i. e. for on-shell external pions only. Consequently, the dependence of the amplitude on the momenta of external pions is not obtained. For instance, to obey the Adler consistency condition [41] $\overline{D}^{+}(\nu = 0, t = \mu^2) = 0$ (with either $k^2 = \mu^2, k'^2 = 0$ or $k^2 = 0, k'^2 = \mu^2$), the σNN vertex and the box graph will have to be dressed in this model, thus requiring an extension to order $\mathcal{O}(a^2)$ in the "analyticity violation expansion" outlined in Section IV.

In the calculation of RBχPT [9] the bulk of the sigma-term at the Cheng-Dashen point comes from a contact four-point vertex in the chiral lagrangian. In the present approach the largest contribution to the sigma-term comes from the tree-level t-channel σ exchange. Due to the scalar component in the $\sigma\pi\pi$ vertex Eq. (A14), the σ exchange contribution does not vanish at the Cheng-Dashen point, thus playing a similar role as the chiral contact term. Nevertheless, the loop contributions are not of minor importance in the near-threshold region: in both this model and in the RBχPT it is through the loops that the essential unitarity, analyticity and crossing constraints are incorporated.

Although the means of regularisation of the loop integrals employed in this model and in the BSE (i. e. the usage of bare form factors) are different to those used in the RBχPT (infrared and dimensional regularisation), they are similar in that they generate spurious singularities of the amplitude. However, in this model and in RBχPT these unwanted singularities are removed from the region of physical interest. For example, the amplitude in the RBχPT has an unphysical pole at $s = 0$, which should be safely far from the relevant near-threshold region [9]. Similarly, the bare form factors in this model are rather wide, and therefore their singularities are located in the complex plane far from the region of physical interest. There is an important difference in the way in which the loop integrals are evaluated in our approach and in the BSE. In the latter method the loops are computed using such techniques as, e. g., the Wick's rotation and Feynman parametrisation, whereas in our framework the loops are calculated through the successive application of the Cutkosky rules and dispersion relations. Although being equivalent in local field theories, these two methods of loop evaluation are likely to differ in cases when the loops are regularised by form factors. Thus analytical properties of the amplitudes dressed in the BSE are probably different to those generated by our approach, which may have important consequences in the near-threshold region.

VI. CONCLUSIONS

A consistent dynamical description of the pion-nucleon amplitude in the near-threshold region should serve as a bridge between the physically accessible low-energy data and chiral low-energy theorems reflecting the QCD dynamics in the nonperturbative regime. In this paper we have shown that essential analyticity constraints can be incorporated in a self-consistent dressing procedure, resulting in a reliable interpolation between the Cheng-Dashen point and threshold. In particular, the pion-nucleon scattering lengths, the nucleon sigma-term and the Adler-Weisberger coefficient C evaluated in our approach are all consistent with the recent data analyses.

In addition to pion-nucleon loops, the approach includes a consistent dressing of the Δ resonance. This allows us to study the role of the Δ for the nucleon sigma-term in more detail than has been done previously. In particular, we found that the contribution of the Δ in the near-threshold region should be considered on par with the even more significant effects of multiple loops. Our dynamical model suggests that effective approaches which go beyond few loop corrections while incorporating the constraints of relativistic invariance, unitarity, crossing symmetry and analyticity can reveal important aspects of the low-energy strong interaction.

ACKNOWLEDGMENTS

I would like to thank Harold Fearing, Andrew Lahiff, Olaf Scholten and Marcello Pavan for stimulating discussions and helpful comments. This work was supported in part by a grant from the Natural Sciences and Engineering Research Council of Canada.

APPENDIX A: CONTRIBUTIONS OF THE ρ AND σ TO THE DRESSING EQUATIONS

The term $\Gamma_I^{\rho\sigma}(p)$ on the right-hand side of Eq. (22) comprises 6 loop diagrams including the ρ and σ degrees of freedom[6],

$$\Gamma_I^{\rho\sigma}(p) = \sum_{n=1}^{3} \Big\{ (\Gamma_I^{\rho})_n(p) + (\Gamma_I^{\sigma})_n(p) \Big\}, \tag{A1}$$

where the different terms are described in the following.

$$(\Gamma_I^{\rho})_1(p) = \frac{1}{8\pi^2} \int d^4k \, \Gamma_\mu^{\rho NN}(k-q, p-k) S_I(p-k) \Gamma_R(p) D_\rho^{\mu\nu}(q-k) \Gamma_\nu^{\rho\pi\pi}(-k, q) D_I(k), \tag{A2}$$

where the $\rho\pi\pi$ vertex has the structure

$$\Gamma_\nu^{\rho\pi\pi}(q, q') = g_{\rho\pi\pi} \left[q'_\nu - q_\nu + \frac{(q^2 - q'^2)(q'_\nu + q_\nu)}{(q+q')^2} \right] F_{\rho\pi\pi}((q+q')^2). \tag{A3}$$

[6]In this appendix we use the notation introduced in Section III.

In order that a converging solution of the dressing should exist, the $\rho\pi\pi$ vertex is equipped with a form factor $F_{\rho\pi\pi}((q+q')^2)$ whose form is the same as that of the bare πNN form factor in Eq. (30),

$$F_{\rho\pi\pi}(k^2) = \exp\left[-\ln 2\frac{(k^2-m_\rho^2)^2}{\Lambda_R^4}\right], \tag{A4}$$

where the half-width Λ_R^2 is given in Table III and discussed in Section III C. Similarly to the treatment of the Δ resonance (see Eq. (18)), we choose a gauge-invariant form of the $\rho\pi\pi$ vertex and therefore retain only the spin 1 part of the ρ propagator

$$D_\rho^{\mu\nu}(k) = \frac{\mathcal{P}_1^{\mu\nu}(k)}{Z^\rho\,[\,k^2-\lambda^2(k^2)\,]}, \tag{A5}$$

with the spin 1 projector

$$\mathcal{P}_1^{\mu\nu}(k) = g^{\mu\nu} - \frac{k^\mu k^\nu}{k^2}. \tag{A6}$$

The ρ self-energy function $\lambda^2(k^2)$ is calculated from one $\pi\pi$ loop as follows:

$$\lambda^2(p^2) = m_\rho^2 - \delta m_\rho^2 + \frac{\mathrm{Re}\Pi_L^\rho(p^2)}{Z^\rho}, \tag{A7}$$

where $\Pi_L^\rho(p^2)$ is the $\pi\pi$ loop contribution to the self-energy and Z^ρ, δm_ρ^2 are real renormalisation constants adjusted to ensure the correct pole properties of the dressed ρ propagator Eq. (A5). As all loop integrals in the model, this loop is evaluated using a dispersion relation:

$$\mathrm{Im}\Pi^\rho(k^2) = -\frac{\mathcal{P}_1^{\nu\mu}(k)}{24\pi^2}\int d^4q\,\Gamma_\mu^{\rho\pi\pi}(q,k-q)D_I(q)D_I(k-q)\Gamma_\nu^{\rho\pi\pi}(q-k,-q)\,, \tag{A8}$$

$$\mathrm{Re}\Pi_L^\rho(k^2) = \frac{\mathcal{P}}{\pi}\int_{4\mu^2}^\infty dk'^2\,\frac{\mathrm{Im}\Pi^\rho(k'^2)}{k'^2-k^2}\,. \tag{A9}$$

The ρNN vertex is chosen as

$$\Gamma_\mu^{\rho NN}(k,p) = g_{\rho NN}\left[\gamma_\mu + i\kappa_\rho\frac{\sigma_{\mu\eta}k^\eta}{2m}\right]F_{\rho NN}(p^2), \tag{A10}$$

where the regularising form factor $F_{\rho NN}(p^2)$ depends on the four-momentum squared of an off-shell nucleon and has the form of Eq. (A4) in which m_ρ is replaced by $m \equiv m_N$. Describing Eq. (A1) further,

$$(\Gamma_I^\rho)_2(p) = \frac{g\gamma_5}{8\pi^3}\int d^4k\,S_I(p-k)\Gamma_\mu^{\rho NN}(-k,p)D(k-q)\Gamma_\nu^{\rho\pi\pi}(-q,q-k)(D_\rho^{\mu\nu})_I(k), \tag{A11}$$

where Eq. (31) has been used;

$$(\Gamma_I^\rho)_3(p) = \frac{1}{32\pi^3}\int d^4k\,\Gamma_\mu^{\rho NN}(k,p'-k)S(p'-k)\overline{\Gamma}_R(p'-k)S_I(p-k)\Gamma_\nu^{\rho NN}(-k,p)(D_\rho^{\mu\nu})_I(k)\,. \tag{A12}$$

The loop integrals with the σ meson have an analogous structure:

$$(\Gamma_I^\sigma)_1(p) = -\frac{g_{\sigma NN}}{8\pi^2}\int d^4k\, S_I(p-k)\Gamma_R(p)D_\sigma(q-k)\Gamma^{\sigma\pi\pi}(-k,q)D_I(k), \tag{A13}$$

where the $\sigma\pi\pi$ vertex is chosen as

$$\Gamma^{\sigma\pi\pi}(q,q') = \left[g_{\sigma\pi\pi}\mu + f_{\sigma\pi\pi}\frac{q\cdot q'}{\mu}\right]F_{\sigma\pi\pi}((q+q')^2). \tag{A14}$$

Similarly to the ρ meson, the σ propagator $D_\sigma(k)$ is obtained from one $\pi\pi$ loop:

$$D_\sigma(k) = \frac{1}{Z^\sigma\,[\,k^2-\zeta^2(k^2)\,]}, \tag{A15}$$

$$\zeta^2(p^2) = m_\sigma^2 - \delta m_\sigma^2 + \frac{\mathrm{Re}\Pi_L^\sigma(p^2)}{Z^\sigma}, \tag{A16}$$

$$\mathrm{Im}\Pi^\sigma(k^2) = -\frac{3}{16\pi^2}\int d^4q\,\Gamma_\mu^{\sigma\pi\pi}(q,k-q)D_I(q)D_I(k-q)\Gamma_\nu^{\sigma\pi\pi}(q-k,-q)\,, \tag{A17}$$

$$\mathrm{Re}\Pi_L^\sigma(k^2) = \frac{\mathcal{P}}{\pi}\int_{4\mu^2}^\infty dk'^2\,\frac{\mathrm{Im}\Pi^\sigma(k'^2)}{k'^2-k^2}\,. \tag{A18}$$

The last two terms in Eq. (A1) read

$$(\Gamma_I^\sigma)_2(p) = \frac{g\gamma_5}{8\pi^3}\int d^4k\, S_I(p-k)\Gamma^{\sigma NN}(-k,p)D(k-q)\Gamma^{\sigma\pi\pi}(-q,q-k)(D_\sigma)_I(k), \tag{A19}$$

$$(\Gamma_I^\sigma)_3(p) = \frac{g_{\sigma NN}^2}{8\pi^3}\int d^4k\,\Gamma^{\sigma NN}(k,p'-k)S(p'-k)\overline{\Gamma}_R(p'-k)S_I(p-k)\Gamma^{\sigma NN}(-k,p)(D_\sigma)_I(k), \tag{A20}$$

where the σNN vertex has the simple structure

$$\Gamma^{\sigma NN}(k,p) = g_{\sigma NN}F_{\sigma NN}(p^2), \tag{A21}$$

with the form factor $F_{\sigma NN}(p^2) = F_{\rho NN}(p^2)$.

The term $(V_\mu^{\rho\sigma})_I(q,p)$ in Eq. (26) comprises two loop integrals whose form is given by Eq. (A2) and Eq. (A13) in which the πNN vertex $\Gamma_R(p)$ is replaced with the $\pi N\Delta$ vertex $(V_\mu)_R(k,p)$.

APPENDIX B: CONTRIBUTION OF THE Δ AT THE CHENG-DASHEN POINT

The contributions of the Δ resonance to the sigma-term and to the coefficient C in Eqs. (41,42) are obtained by decomposing Eqs. (37,38) into the invariant amplitudes $D^{\pm}$ and evaluating the latter at the Cheng-Dashen point. The expressions in terms of the dressed $\pi N\Delta$ form factor and the dressed Δ self-energy functions, defined in Eqs. (16,19), are

$$\Sigma_\Delta = -\frac{2F_\pi^2 G_\Delta^2(m^2)\,\omega(m^2)}{9\,m_\Delta^4\eta(m^2)[\,m^2-\omega^2(m^2)\,]}\,\mu^4\,, \tag{B1}$$

$$\begin{aligned} C_\Delta = {} & \frac{8F_\pi^2 m\omega(m^2)G_\Delta^2(m^2)}{9\,m_\Delta^4\eta(m^2)[\,m^2-\omega^2(m^2)\,]}\,\mu^2 \\ & + 2F_\pi^2\left\{\frac{G_\Delta^2(m^2)+4m\omega(m^2)G_\Delta(m^2)G'_\Delta(m^2)}{9m_\Delta^4\eta(m^2)[\,m^2-\omega^2(m^2)\,]} - \frac{2mG_\Delta^2(m^2)\eta(m^2)\omega(m^2)}{9m_\Delta^4\eta^2(m^2)[\,m^2-\omega^2(m^2)\,]^2}\right. \\ & \left. + \frac{2mG_\Delta^2(m^2)[\,m^2+\omega^2(m^2)\,]\,[\,\eta(m^2)\omega'(m^2)-\omega(m^2)\eta'(m^2)\,]}{9m_\Delta^4\eta^2(m^2)[\,m^2-\omega^2(m^2)\,]^2}\right\}\mu^4\,, \end{aligned} \tag{B2}$$

explicitly showing the suppression by powers of the pion mass μ.

TABLES

TABLE I. Particle masses (in GeV) and coupling constants used in this calculation (the same values were used in Ref. [14]). The masses and the coupling constants of the Δ, ρ and σ correspond to the experimental widths and positions of the resonances as given in [18].

$m \equiv m_N$	$\mu \equiv m_\pi$	m_Δ	m_ρ	m_σ	$g \equiv g_{\pi NN}$	$g_{\pi N\Delta}$
0.939	0.138	1.232	0.77	0.76	13.02	19.76

TABLE II. The renormalisation parameters: bare coupling constants, mass shifts (in units of GeV) and field renormalisation factors.

$f \equiv f_{\pi NN}$	$f_{\pi N\Delta}$	$\delta m \equiv \delta m_N$	δm_Δ	δm_ρ^2	δm_σ^2	$Z_2 \equiv Z_2^N$	Z_2^Δ	Z^ρ	Z^σ
10.75	21.75	-0.075	-0.120	-0.089	-0.605	0.80	1.16	1.17	1.14

TABLE III. The values of the parameters of the model, as fixed by calculating the intermediate-energy pion-nucleon phase shifts in the dressed K-matrix approach of Ref. [14]. No parameters were adjusted in this calculation.

Λ_N^2	Λ_R^2	$g_{\rho NN}$	κ_ρ	$g_{\sigma NN}$	$g_{\sigma\pi\pi}$	$f_{\sigma\pi\pi}$
1.8	1.0	7.0	2.3	34	1.7	1.8

TABLE IV. The pion-nucleon sigma-term, the Adler-Weisberger coefficient C, evaluated at the Cheng-Dashen point from Eqs. (3,8), and the s-wave scattering lengths, evaluated from Eqs. (9,10). The following five calculations are presented. Column 1: the fully dressed calculation; column 2: the full calculation, but without the s- and u-channel Δ exchange pole diagrams; column 3: the full calculation, but without the consistent dressing of the Δ propagator and $\pi N\Delta$ vertex; column 4: the calculation in which the nucleon, Δ self-energies and the πNN, $\pi N\Delta$ vertices are computed up to one-loop corrections only; column 5: the bare calculation, i. e. using the free propagators and no loop corrections to the bare vertices; column 6: results of various data analyses.

	Dressed	No Δ poles	Bare Δ	One loop	Bare	Data analyses
Σ (MeV)	73.99	73.73	74.05	71.98	127.78	64 ± 8 [29]
						79 ± 7 [30]
						71 ± 9 [7]
C	1.16	1.21	1.14	1.21	1.31	1.15 ± 0.02 [29]
$a^{1/2}(\mu^{-1})$	0.175	0.175	0.175	0.181	0.204	0.173 ± 0.0003 [22]
						0.175 ± 0.0041 [31]
$a^{3/2}(\mu^{-1})$	-0.087	-0.087	-0.087	-0.093	-0.088	-0.101 ± 0.0004 [22]
						-0.085 ± 0.027 [31]

TABLE V. Comparison of the near-threshold parameters evaluated in the present model with results obtained in chiral perturbation theory and in the approach based on the Bethe-Salpeter equation. The third and fourth order calculations [33] in the heavy-baryon chiral perturbation theory (HBχPT) presented fits to three different phase-shifts, using Ref. [7] to relate the sigma-term and threshold parameters. The relativistic infrared-regularised baryon approach (RBχPT) [9] used the data analyses of [29] as input. The Bethe-Salpeter equation (BSE) calculation is from Ref. [10].

	This model	HBχPT $\mathcal{O}(p^3)$	HBχPT $\mathcal{O}(p^4)$	RBχPT $\mathcal{O}(p^4)$	BSE
Σ (MeV)	73.99	69	73	61	23.6
		91	85		
		93	104		
C	1.16	1.10		1.13	
		0.82			
		1.09			
$a^{1/2}(\mu^{-1})$	0.175	0.171	0.171	0.175	0.177
		0.159	0.159		
		0.175	0.176		
$a^{3/2}(\mu^{-1})$	-0.087	-0.101	-0.100	-0.100	-0.101
		-0.072	-0.073		
		-0.086	-0.084		

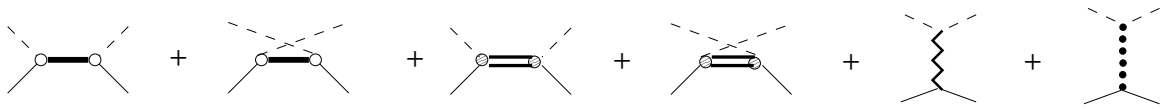

FIG. 1. Graphical representation of the pion-nucleon amplitude, corresponding to Eq. (11). The single solid lines are nucleons, the double lines are Δ's, the dashed, zigzag and dotted lines are pions, ρ's and σ's, respectively. The empty and hatched circles denote the πNN and $\pi N\Delta$ vertices, respectively. The propagators and vertices are dressed with meson loops as described in Section III C.

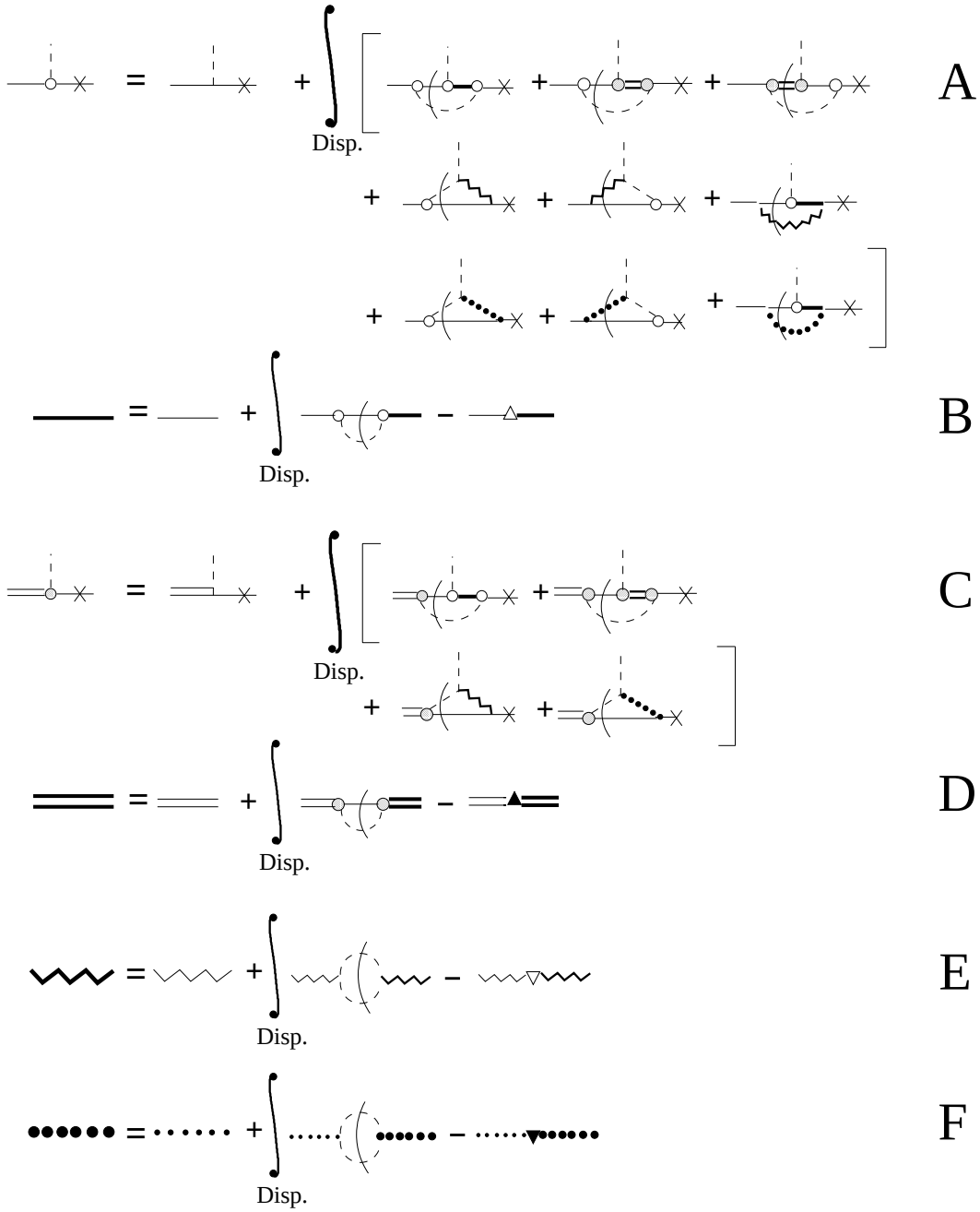

FIG. 2. Graphical representation of the system of integral equations for the dressed two- and three-point Green's functions. The notation for the propagators and vertices is as in Fig. 1. For each particle, the dressed and free propagators are denoted by thick and thin lines, respectively. The triangles denote the counterterms needed to fulfill the renormalisation conditions such as Eq. (32). The slashes through the loops and the integral signs indicate the use of the cutting rules and dispersion integrals in the iterative solution of the equations. The outgoing nucleons in the vertices (as well as the pions) are on-shell, which is denoted by the crossed lines. The correspondence with analytic equations is **A** $\leftrightarrow (22, 23)$, **B** $\leftrightarrow (24, 25)$, **C** $\leftrightarrow (26, 27)$, **D** $\leftrightarrow (28, 29)$, **E** $\leftrightarrow (A8, A9)$, **F** $\leftrightarrow (A17, A18)$.

REFERENCES

[1] S. Weinberg, Phys. Rev. Lett. **17**, 616 (1966).

[2] S.L. Adler, Phys. Rev. **140**, B736 (1965); W.I. Weisberger, Phys. Rev. **143**, 1302 (1966).

[3] T.P. Cheng and R. Dashen, Phys. Rev. Lett. **26**, 594 (1971); L.S. Brown, W.J. Pardee, and R.D. Peccei, Phys. Rev. D **4**, 2801 (1971).

[4] E. Reya, Rev. Mod. Phys. **46**, 545 (1974).

[5] J.F. Donoghue and C.R. Nappi, Phys. Lett. B **168**, 105 (1968); R.L. Jaffe and C.L. Korpa, Comm. Nucl. Part. Phys. 17, 163 (1987); R.D. Ball, S. Forte, and J. Tigg, Nucl. Phys. B **428**, 485 (1994).

[6] J. Gässer, H. Leutwyler, M.P. Locher and M.E. Sainio, Phys. Lett. B **213**, 85 (1988); J. Gässer, H. Leutwyler, and M.E. Sainio, Phys. Lett. B **253**, 252 (1991); *ibid.*, Phys. Lett. B **253**, 260 (1991).

[7] M.G. Olsson, Phys. Lett. B **482**, 50 (2000).

[8] J. Gasser, Ann. of Phys. **136**, 62 (1981); J. Gasser and H. Leutwyler, Phys. Rev. **87**, 77 (1982); B. Borasoy and Ulf-G. Meissner, Ann. of Phys. **254**, 192 (1997); M. Knecht, PiN Newslett. **15**, 108 (1999); B. Borasoy, Eur. Phys. J. C **8**, 121 (1999); J. Gässer and M.E. Sainio, hep-ph/0002283; M.E. Sainio, hep-ph/0110413.

[9] T. Becher and H. Leutwyler, J. High En. Phys. **0106**, 017 (2001); Eur. Phys. J. C **9**, 643 (1999).

[10] A.D. Lahiff and I.R. Afnan, Phys. Rev. C **60**, 024608 (1999); I.R. Afnan and A.D. Lahiff, in preparation.

[11] M.F.M. Lutz and E.E. Kolomeitsev, Nucl. Phys. A **700**, 193 (2002).

[12] S. Kondratyuk and O. Scholten, Phys. Rev. C **59**, 1070 (1999); *ibid.*, Phys. Rev. C **62**, 025203 (2000).

[13] S. Kondratyuk and O. Scholten, Nucl. Phys. A **677**, 396 (2000).

[14] S. Kondratyuk and O. Scholten, Phys. Rev. C **64**, 024005 (2001).

[15] S. Kondratyuk and O. Scholten, Phys. Rev. C **65**, 038201 (2002).

[16] G.F. Chew, M.L. Goldberger, F.E. Low, and Y. Nambu, Phys. Rev. **106**, 1337 (1957).

[17] A.Yu. Korchin, O. Scholten, and R. Timmermans, Phys. Lett. B **438**, 1 (1998).

[18] Particle Data Group, D.E. Groom *et al.*, Eur. Phys. J. C **15**, 1 (2000).

[19] E. Kazes, Nuovo Cimento **13**, 1226 (1959).

[20] J.D. Bjorken and S.D. Drell, *Relativistic Quantum Mechanics* (McGraw-Hill, 1964); *ibid.*, *Relativistic Quantum Fields* (McGraw-Hill, 1965).

[21] S. Weinberg, *The Quantum Theory of Fields* (Cambridge University Press, 1996), ch. 10.

[22] T. Ericson and W. Weise, *Pions and Nuclei* (Oxford, 1988).

[23] V. Pascalutsa, Phys. Rev. D **58**, 096002 (1998); *ibid.* Phys. Lett. B **503**, 85 (2001).

[24] W. Rarita and J. Schwinger, Phys. Rev. **60**, 61 (1941); M. Benmerrouche, R.M. Davidson, and N.C. Mukhopadhyay, Phys. Rev. C **39**, 2339 (1989).

[25] C.L. Korpa, Heavy Ion Physics **5**, 77 (1997).

[26] R.E. Cutkosky, J. Math. Phys. **1**, 429 (1960); M. Veltman, Physica 29, 186 (1963).

[27] N.N. Bogoliubov and D.V. Shirkov, *Introduction to The Theory of Quantized Fields* (Interscience, New York, 1959); G. Barton, *Dispersion Techniques in Field Theory* (Benjamin, New York, 1965); A. Bincer, Phys. Rev. **118**, 855 (1960).

[28] R.A. Arndt, I.I. Strakovskii, and R.L. Workman, Phys. Rev. C **52**, 2120 (1995); *ibid.*, Phys. Rev. C **53**, 430 (1996).

[29] G. Höhler, *Pion-Nucleon Scattering*, Landolt-Börnstein, 1/9b2, ed. H. Schopper (Springer, 1983); R. Koch, Z. Phys. C15, 161 (1982).
[30] M.M. Pavan *et al.*, hep-ph/0111066.
[31] H.-Ch. Schröder *et al.*, Phys. Lett. B **469**, 25 (1999).
[32] V. Bernard, N. Kaiser, and Ulf-G. Meissner, Int. J. Mod. Phys. **E4**, 193 (1995).
[33] N. Fettes, Ulf-G. Meissner, and S. Steininger, Nucl. Phys. A **640**, 199 (1998); N. Fettes and Ulf-G. Meissner, Nucl. Phys. A **676**, 311 (2000).
[34] V. Bernard, N. Kaiser, and Ulf-G. Meissner, Z. Phys. C60, 111 (1993); T.R. Hemmert, B.R. Holstein, and J. Kambor, Phys. Rev. D **57**, 5746 (1998).
[35] V. Bernard, N. Kaiser, and Ulf-G. Meissner, Phys. Lett. B **389**, 144 (1996).
[36] H.W. Fearing, Few Body Syst. Suppl. 12 (2000) 263; S. Kondratyuk, A.D. Lahiff, and H.W. Fearing, Phys. Lett. B **521**, 204 (2001).
[37] G. Ecker, J. Gasser, A. Pich, and E. De Rafael, Nucl. Phys. B **321**, 311 (1989).
[38] S. Weinberg, Physica A **96**, 327 (1979); J. Gasser and H. Leutwyler, Ann. of Phys. **158**, 142 (1984); J. Gasser, M.E. Sainio, and A. Svarc, Nucl. Phys. B **307**, 779 (1988); G. Ecker, Prog. Part. Nucl. Phys. **35**, 1 (1995); J. Gasser, Nucl. Phys. Proc. Suppl. **86**, 257 (2000).
[39] E. Jenkins and A.V. Manohar, Phys. Lett. B **255**, 558 (1991); V. Bernard, N. Kaiser, J. Kambor, and Ulf-G. Meissner, Nucl. Phys. B **388**, 315 (1992).
[40] E.F. Salpeter, H.A. Bethe, Phys. Rev. **84**, 1232 (1951); M.M. Broido, Rep. Prog. Phys. **32**, 493 (1969).
[41] S. Adler, Phys. Rev. **137**, 1022 (1965).